Gamma-Ray and Conversion-Electron Spectroscopy of Exotic Heavy Nuclei

Rauno Julin

Department of Physics, University of Jyväskylä, P.O.B. 35 (JYFL), 40351 Jyväskylä, Finland

Abstract. The main principles of gamma-ray and conversion-electron spectrometry are discussed. Examples are presented where tagging methods are employed in gamma-ray and electron-spectroscopic studies of nuclei close to the proton drip-line of $Z \approx 82$ nuclei and trans-fermium nuclei near $Z = 102$.

1 Introduction

One of the goals of nuclear structure physics is to understand various modes of nuclear excitations. A dominant part of de-excitations of nuclear excited states proceeds via γ-ray emission. Therefore, it is obvious that γ-ray spectroscopy provides one of the most powerful methods for nuclear structure studies. Moreover, the fact that a γ ray can penetrate a layer of material without any interaction i.e. without any energy loss or energy straggling, enables high-precision spectroscopy. In addition to the energy information, the emission sequence, time relationships as well as electromagnetic properties of γ rays give information about the nuclear structure changes when the nucleus loses energy and angular momentum.

Structure studies of exotic nuclei in the drip-line and super-heavy regions are a new challenge for nuclear spectroscopy. These nuclei are produced using exotic beams or very weak reaction channels. Therefore, in addition to high-efficiency γ-ray detector arrays in such studies, powerful channel selection devices are needed for resolving the rare events of interest from the background originating from other dominant reaction channels or radioactivity.

For low-energy electromagnetic transitions and for E0 transitions in heavy nuclei internal electron conversion is a dominant de-excitation mode. Therefore, it is obvious that methods for detecting electrons in in-beam and off-beam measurements are called for.

In the following section the main principles of γ-ray and conversion-electron spectroscopy are discussed. Examples are presented, where tagging methods are employed in γ-ray and electron-spectroscopic studies of nuclei close to the proton drip-line of $Z \approx 82$ nuclei and trans-fermium nuclei near $Z = 102$. These experiments were carried out in the Accelerator Laboratory of the Department of Physics of the University of Jyväskylä (JYFL), Finland.

R. Julin, Gamma-Ray and Conversion-Electron Spectroscopy of Exotic Heavy Nuclei, Lect. Notes Phys. **651**, 263–294 (2004)
http://www.springerlink.com/

2 Production of Nuclear Excited States

Yrast and non-yrast states. A goal in experimental studies of low-lying nuclear excited states is what is called "complete spectroscopy", which means that all excited states up to a certain excitation energy are identified and studied. The resulting data are a challenge when testing various nuclear models. With increasing excitation energy the level density and mixing of different configurations quickly increases. Only close to the yrast line (the line of the lowest energy of certain spin) i.e. at low temperature, can discrete levels of relatively pure configuration be observed (Fig. 1). Discrete γ-ray lines from high-spin states up to $I \approx 60\,\hbar$ at the yrast line in medium-heavy nuclei have been observed. The maximum available spin in heavy nuclei is obviously limited by fission. Higher above the yrast line i.e. at higher temperature, nuclei in the continuum states are typically de-excited towards the yrast line by fast dipole transitions forming a continuum spectrum of γ rays.

In-beam and off-beam measurements. De-excitation of nuclear excited states via emission of cascades of γ rays or conversion electrons to the ground state proceeds typically within a nanosecond. Therefore, if these excited states are

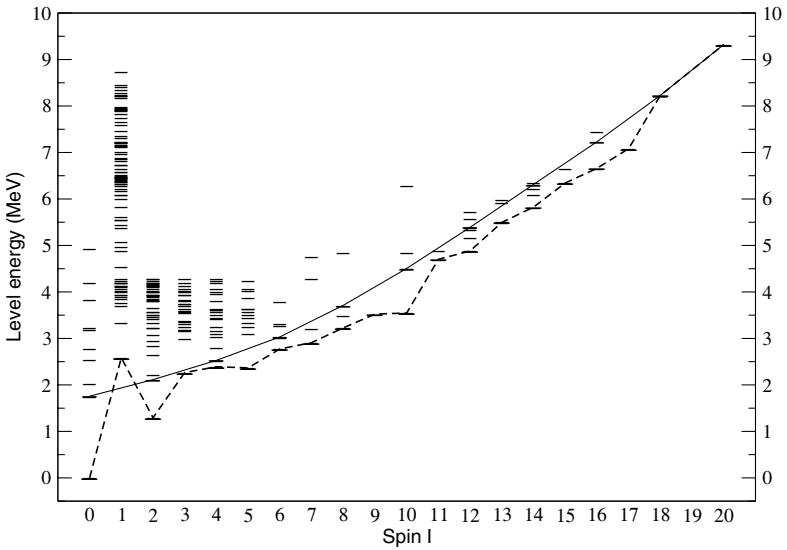

Fig. 1. Yrast plot for experimentally observed excited states of the neutron mid-shell nucleus ^{116}Sn [1]. The irregular yrast line (*dashed line*) up to 7 MeV ($I = 17$) is due to spherical states of irregular level spacing. The observed members of an intruder band are connected with a solid line. This band with regular level spacing and becoming yrast above 7 MeV is associated with a coexisting deformed structure. Availability of stable-isotope target nuclei close to ^{116}Sn enable observation of a large number of low-spin states via light-ion induced reactions

directly produced in nuclear reactions, the emitted γ rays or electrons must be detected close to the target in an *in-beam* measurement. De-excitation of states populated in the β or α decay, or long-living isomeric states, can be studied in *off-beam* measurements, typically following a possible separation of the decaying nuclei of interest.

Close to and far from the line of stability. Nuclei close to the valley of stability can be produced in excited states via many types of light- and heavy-ion induced reactions or via β decay. The goal of modern nuclear spectroscopy is to extend systematic spectroscopic studies far from the stability line towards the drip lines and super-heavy nuclei. Production of these exotic nuclei is limited by the available nuclear reactions.

Neutron deficient nuclei via fusion evaporation. Fusion-evaporation reactions with stable-isotope heavy-ion beams and stable-isotope targets can be used to produce neutron deficient nuclei close to the proton drip-line and also to produce very heavy nuclei. However, due to the increasing number of open evaporation channels when the neutron number decreases or due to increasing fission cross-section when going to heavy nuclei, the fusion cross-sections quickly drop down. Therefore, tagging methods by combining in-beam and off-beam gamma-ray and electron detection with high-efficiency channel selection are needed.

Neutron-rich nuclei. Due to the fact that the neutron excess of bound nuclei increases with their mass, the fusion evaporation with stable-isotope beams and targets cannot be used to produce neutron-rich nuclei. Gamma-ray detection from incomplete fusion and transfer-reaction products or from fission fragments can be used to probe levels up to intermediate spin in nuclei a few neutrons away from the stability line. Most of the spectroscopic information for neutron-rich medium-heavy nuclei is still obtained from studies of β-decaying fission fragments and their decay products.

Radioactive beams. The availability of radioactive beams has opened up new possibilities for studies of exotic nuclei far from stability. Low-energy beams of radioactive nuclei produced by using ISOL methods and high-energy beams of nuclei produced by employing nuclear fragmentation can be Coulomb excited in a target of heavy isotopes. The separated radioactive species can also be stopped for decay measurements. Intense radioactive beams can be used to induce fusion-evaporation reactions. In spectroscopic studies with radioactive beams spectrometers of high efficiency and high resolving power are needed. For most of the measurements they must be combined with other ancillary devices similar to those used in studies of exotic nuclei produced via weak reaction channels with stable-isotope beams.

3 Gamma-Ray Spectrometers

3.1 Detector

Ge detector. A major step forward in nuclear spectroscopy was taken with the development of Ge semiconductor detectors. Very good energy resolution (approx. 1 keV at 120 keV and 2 keV at 1 MeV) can be obtained with these detectors. From 1960's to the end of 1970's lithium drifted Ge(Li) detectors were used. In 1980's the Ge(Li) detectors were replaced by the detectors made out of hyperpure germanium. Today the largest single-crystal Ge detectors (open-end coaxial type) have a depletion region of almost one litre. Photopeak efficiency of a large-volume Ge detector is close to that of the standard $3'' \times 3''$ NaI(Tl) scintillation detector ($1.2 \cdot 10^{-3}$ or 0.12 % at 1.3 MeV for a detector at a distance of 25 cm from the source).

Compton suppression. The Ge detectors still suffer from the relatively poor peak-to-background ratio, mainly caused by γ rays Compton scattered out of the Ge crystal. Even with the largest Ge crystals approximately 80 % of the observed counts are in the Compton tail. This tail is especially harmful in in-beam measurements when the γ-ray spectra are very complicated. It can be reduced by employing a Compton-suppression shield surrounding the Ge detector (Fig. 2a). The first suppression shields were large NaI(Tl) scintillation detectors. In the mid 1980's a denser scintillation material, bismuth germanate (BGO), became available and enabled construction of compact

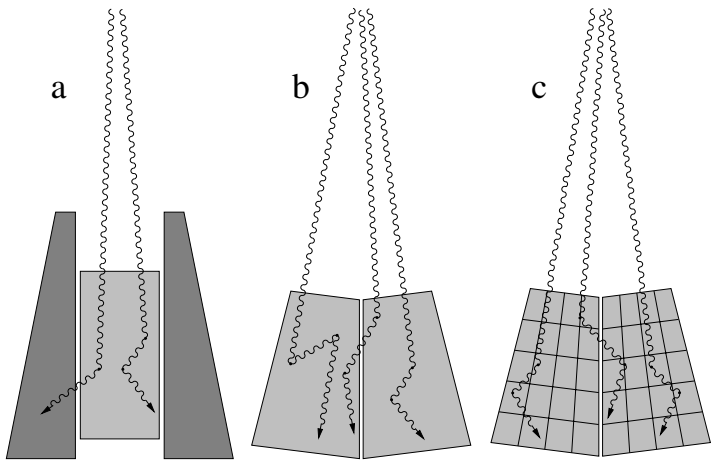

Fig. 2. (**a**) An active Compton-suppression shield surrounding the Ge detector is used to veto events partially absorbed in the Ge crystal. (**b**) Signals from Compton events detected by the Ge crystals of a composite detector can be added (adding-back mode). (**c**) Segmentation of the composite detectors enables reconstruction of tracks of individual γ rays

suppression shields and consequently, construction of compact Ge-detector arrays with high resolving power.

Composite detectors. More efficient Ge-detector arrays are needed for gamma-ray studies at very low production rates. As the size of a Ge-crystal is limited, this cannot be done by using the single crystal detectors. Therefore, for covering a large solid angle with active Ge-detector material, composite detectors are needed (Fig. 2b). The most common type nowadays in use is the Clover detector composed of four Ge crystals in one cryostat. Another solution is to use cluster detectors composed of encapsulated Ge crystals.

Segmented detectors. In in-beam and off-beam γ-ray spectroscopy high granularity (number of individual detector elements) of the detector array is advantageous. Therefore, the new arrays are composed of detectors with segmented Ge crystals. Each of the segments of the Ge crystal works as an individual detector. The segmented Ge detectors and pulse-shape analysis of the segment signals using digital electronics are the basis for a new concept in γ-ray spectroscopy, γ-ray tracking. The ultimate goal is to cover 80 % of the 4π solid angle with active Ge-detector material and select only full-absorption events by reconstructing tracks of individual γ rays (Fig. 2c).

3.2 Principles of Gamma-Ray Detection

A γ-ray spectrometer to study exotic nuclei should be capable of measuring γ radiation in a large energy range, from a few tens of keV up to 10 MeV with high efficiency and with good spectral response. This requires a simultaneous optimisation of several and often conflicting properties.

Doppler effects. Best energy resolution can be obtained for γ rays emitted by nuclei in rest. This is the case in off-beam spectroscopy of radioactive species. For the in-beam measurements reaction products can also be stopped by using thick targets or targets with backing material. However, sharp lines are then observed only for transitions from the states with lifetimes longer than the stopping time of the recoil. This time depends on the velocity of the recoil, being typically around 0.5 picoseconds.

For γ rays emitted by a moving source a Doppler-shift is observed (Fig. 3). The γ-ray energy is determined by the formula:

$$E_\gamma = E_0(1 + \frac{v}{c}\cos\theta) \; . \tag{1}$$

Where E_0 is the transition energy, v is the speed of the recoil, c is the speed of light and θ the angle between the emission direction of the γ ray and the direction of the velocity vector of the emitting nuclear recoil. In

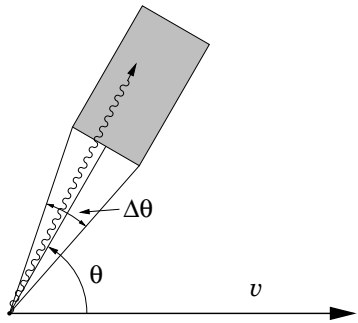

Fig. 3. An energy measurement of γ rays emitted by moving recoils is disturbed by Doppler effects. The Doppler shift depends on the detection angle and the Doppler broadening on the opening angle of the detector

studies of exotic nuclei v/c can be as high as 0.5 for reactions at relativistic energies, like fragmentation and Coulomb excitation. For the exotic recoils from fusion-evaporation reactions induced by projectile energies close to the Coulomb barrier, v/c is 0.01–0.10 depending on the symmetry of the reaction.

When the target is thin enough so that the γ rays of interest are emitted by flying recoils outside the target, the Doppler-shift can be corrected in the data analysis if the angle θ is known. For this information the recoiling nucleus or the scattered projectile must be detected by using a position sensitive detector. For fusion evaporation reaction an assumption can be made that the recoils are all flying to forward direction along the beam axis. The γ-ray detection angle is determined by the location of the γ-ray detector.

Due to the finite opening angle $\Delta\theta$ of the detector with respect to the recoil-velocity direction, a Doppler-broadening of γ rays is observed (Fig. 3):

$$\Delta E_\gamma = E_0 \frac{v}{c} \sin\theta \, \Delta\theta \; . \tag{2}$$

For example, for a 1 MeV γ rays emitted by recoils of $v/c = 0.05$ and detected by a γ-ray detector of 5 cm in diameter at an angle of 90 degrees with respect to the recoil velocity and at a distance of 20 cm from the recoil, the broadening is around 10 keV. Consequently, it is obvious that the detector array for in-beam measurements must have a good angular resolution i.e. the granularity of the array must be high enough.

Multiple hits. Granularity is also needed to avoid multiple hits of a single detector element by more than one γ ray of a cascade of γ rays emitted in the decay of an excited state (Fig. 4). The γ-ray multiplicity M_γ (the number of γ-ray transitions in the cascade) can be high in in-beam measurements, especially in fusion-evaporation reactions, occasionally reaching $M_\gamma \approx 30$. In decay measurements it is limited to 1–5.

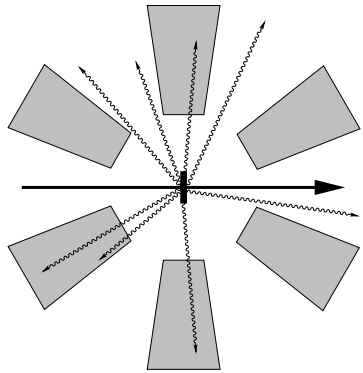

Fig. 4. Minimum distance of the γ-ray detectors from the source or the target is limited by the probability of a simultaneous detection of more than one γ ray (multiple hit) of a γ-ray cascade by a single detector

For example, for a $\oslash = 5\,cm$ detector at a distance of 15 cm the probability to detect simultaneously two γ rays from a cascade of 10 γ rays is approximately 6 %. In the γ-ray spectrum these events are falling outside the full energy photo peak, increasing the contribution of the continuous background and sum peaks.

Counting rate. The length of the energy signal from a linear amplifier with a typical shaping time of 2 µs is approximately 12 µs. To avoid losses due to random piling up of these signals the maximum counting rate limit of a single detector is typically set to about 10^4 counts/sec. By deriving a time signal with amplitude and rise time compensation the pile-up events down to about 100 ns in time difference can be rejected. Rate limits are also set by the dead time of most of the presently used data acquisition systems. The maximum rate set by a single detector is one of the reasons for using high-granular multi-detector arrays.

The counting rate limit set by the Ge detectors is one of the most severe limitations in in-beam studies of exotic nuclei. The total cross-section for nuclear reactions induced by any projectile with a bombarding energy above the Coulomb barrier is close to 1 barn. A typical target thickness, enabling recoiling reaction products to emit γ rays in flight, is usually approximately 0.5 mg/cm^2. Therefore, in practice the total γ-ray yield is such that with a standard large Ge detector at a distance of 20 cm from the target the counting rate limit of 10^4 counts/sec is reached with a beam current of approximately 10 particle-nA. The examples discussed in Sect. 6 show that with such beam currents the observation limit in in-beam γ-ray measurements represents a cross-section for the channel of interest of the order of 100 nb when recoil decay tagging methods are used. In terms of reaction rate it is only about 40 reactions per hour !

In off-beam decay studies at the focal plane of the separators, the radiation from the disturbing reaction channels is minimised and therefore the production of nuclei of interest is typically limited by the target durability or the beam intensity available from the accelerator.

In the near future digital signal processing electronics will be further developed. In order to preserve all the relevant features of the preamplifier signal of a Ge detector, it will be digitised with at least 12-bit resolution. In addition to γ-ray tracking, this will also enable, at least in principle, to increase the counting rate of a Ge detector up to 10^5 counts/sec.

Peak-to-total ratio and detection efficiency. After selection of the reaction channel of interest and rejection of the multiple-hit and pile-up events it is finally important to maximise the ratio of the total absorption photo-peak events to the total number of events generated by the γ rays (peak-to-total ratio = P/T). In practice, P/T values of 0.5 can be obtained by using a single crystal detector with a BGO Compton-suppression shield (Fig. 2a). With composite Ge detectors similar P/T values are reached when in addition to the Compton-suppression shield of the detector cluster, Compton events detected by two adjacent crystals are added (adding-back mode). However, a clever algorithm or digital signal analysis is needed to resolve Compton events from those generated by two different gamma rays from a cascade.

Especially, when detecting γ rays from exotic nuclei, it is very rarely when low detection efficiency can be compensated by increasing the source strength or beam intensity. Moreover, for a construction of energy level schemes, coincidence information is needed. The probability of simultaneous detection of two coincident γ rays from a cascade is related to the square of the detection efficiency of the array, providing that the granularity of the array is high enough to keep the rate of multiple hits low. Also the high P/T ratio is stressed in coincidence measurements: While the total absorption events are concentrated in the photo peak, the Compton events represent a continuous distribution and are in a two-fold coincidence measurement distributed over a two-dimensional plane. Therefore, for example, a Compton-suppression factor of 3 in the singles spectrum can be thought to be $3^2 = 9$ in a coincidence measurement. The factor is $3^3 = 27$ if triple coincidence events are detected.

3.3 Gamma-Ray Detector Arrays

In the past, the development of γ-ray detector arrays was driven by conditions set by high-spin spectroscopy, while in decay studies of low-spin states close-geometry setup, typically of two bare Ge detectors were used. Today the communities of high-spin and low-spin spectroscopy have merged and modular arrays are designed for obtaining high-quality spectra in both types of measurements. Moreover, arrays designed for studies of exotic nuclei are often meant to be combined with ancillary detectors and separators for a selection

of weak reaction channels in a hostile environment of intense background radiation.

First attempts to push towards higher spin were made in the beginning of 80's when the Spin Spectrometer of 72 segmented NaI(Tl) detectors at Oak Ridge National Laboratory [2] and the Crystal Ball of 162 similar detectors at Max-Planck-Institute in Heidelberg [3] were constructed. Soon after that BGO scintillation material became available. The first arrays of Ge detectors with BGO Compton-suppression shields turned out to be superior in high-spin spectroscopy. One of the earliest of these arrays, the TESSA3 array at the Daresbury Laboratory in UK [4], was used in the discovery of a discrete super-deformed (SD) band in ^{162}Dy [5]. The TESSA3 array consisting of 16 Compton suppressed Ge detectors, each having a photo-peak efficiency of 25 % of that for the $3'' \times 3''$ NaI(Tl) scintillation detector at 1.3 MeV. The total photo-peak efficiency of the TESSA3 array was only about 0.5 % (0.005) at 1.3 MeV, but with its multiplicity filter of 64 BGO crystals it had a high resolving power in high-spin spectroscopy.

Several arrays of 1 % in efficiency were constructed and successfully used in the late 80's in Europe and in the USA. In the 1990's the EUROGAM (Daresbury, UK) [6], GASP (Legnaro, Italy) [7] and the early implementation of GAMMASPHERE (Berkeley, USA) [8] arrays were constructed . These arrays consisted of 40–50 large volume single Ge-crystal detectors (70 % in eff.) with BGO shields and had a total photo-peak efficiency of $\approx$ 5 % at 1.3 MeV.

By the end of the last millennium the most powerful Ge-detector arrays of up to 10 % in efficiency were GAMMASPHERE and EUROBALL, designed primarily for high-spin spectroscopy. GAMMASPHERE is composed of 110 single-crystal Compton-suppressed Ge detectors [8]. EUROBALL consists of 15 Compton suppressed Cluster detectors (7 encapsulated Ge crystals), 26 Compton suppressed Clover detectors and 30 Compton suppressed EUROGAM Phase 1 Ge-detectors adding up to a total of 239 Ge crystals [9] (Fig. 5).

The new exciting perspectives at the radioactive beam facilities have triggered development programmes for more efficient Ge-detector arrays. The aim is to increase the detection efficiency by covering a larger portion of the total solid angle by Ge material and maintain the good energy resolution and high P/T ratio by employing segmented Ge crystals. The EXOGAM array, to be mainly employed at GANIL in France, will consist of 16 Compton suppressed Clover detectors each composed of four four-fold segmented large Ge crystals (60 mm diameter, 90 mm length) [10] (Fig. 6). Two detector configurations of the 16 detectors will be used. The close geometry setup for low-multiplicity experiments should give a total peak efficiency at 1.3 MeV of as high as 20 % in the adding-back mode.

The MINIBALL array has been designed for low-multiplicity experiments with radioactive beams from the REX-ISOLDE facility at CERN. It will

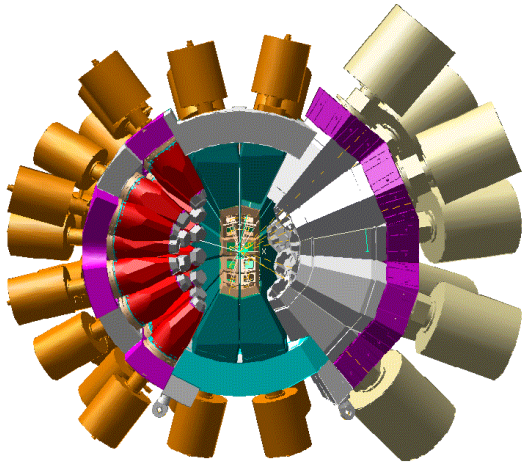

Fig. 5. Section view of the EUROBALL array

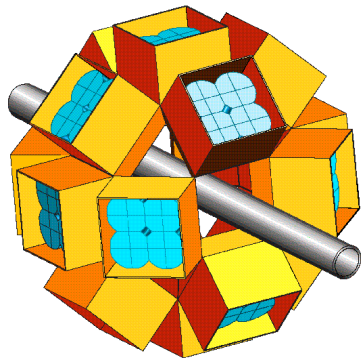

Fig. 6. The EXOGAM array of 16 Compton-suppressed Clover detectors

consist of 40 six-fold segmented, encapsulated Ge detectors clustered in eight cryostats with three detectors and four cryostats with four detectors [11].

New developments towards γ-ray tracking have been started by constructing prototype detectors with additional segmentation in depth and by using pulse-shape analysis. In the framework of the GRETA project the Berkeley group has shown that a position sensitivity of about 1 mm can be achieved with a 36-fold segmented Ge-detector [12]. The Padova group is using a 25-fold segmented Ge-detector and comparing its performance with extensive Monte-Carlo simulations [13].

Advanced Gamma Tracking Array (AGATA) is a joint European project for development of a highly-segmented multipurpose Ge detector array [14]. The main building block of AGATA is a hexagonal, 36-fold (6 times in depth) segmented encapsulated Ge crystal (70 mm diameter, 100 mm length). Three

of such detectors with digital front-end electronics and a common LN_2 dewar form an AGATA module. A close packed spherical AGATA array consists of 60 of such modules.Development of digital signal-processing electronics and a pulse-shape analysis algorithm for real-time applications are essential parts of the AGATA project.

All the developments of the aforementioned segmented large Ge detectors are based on the use of coaxial crystals. However, a development program is foreseen for studying possibilities of constructing a high-granular large Ge detector by using a stack of segmented planar detectors. Such position sensitive planar detectors can also be used for other applications in γ-ray spectroscopy. One of the detectors of the GREAT spectrometer at the focal plane of the RITU gas-filled separator in Jyväskylä, Finland, is a 1.5 cm thick, 12×24 segmented planar Ge detector, used to obtain high-resolution for delayed low-energy γ rays and to detect electrons and positrons from β decay [15].

4 Conversion-Electron Spectrometers

4.1 Internal Conversion

Nuclear electromagnetic transitions can also proceed via internal electron conversion. However, in general, high resolution spectroscopy with electrons is much more difficult than that with γ rays. It is also difficult to construct a multipurpose electron-detector array similar to a Ge-detector array.

Internal conversion increases with increasing Z, decreasing transition energy and increasing multipolarity of the transition. Internal conversion in light and medium-heavy nuclei is weak and dominates only for very low-energy transitions and electric monopole (E0) transitions. However, as shown in Fig. 7, internal conversion is a dominant de-excitation mode for low-energy transitions in heavy nuclei. Therefore, off-beam and in-beam spectroscopic methods are clearly required for detection of electrons from heavy nuclei to complement γ-ray measurements.

Electric monopole transitions between low-lying 0^+ states in nuclei near the line of stability were extensively studied by a JYFL group in Jyväskylä by using in-beam electron-spectroscopic methods with light-ion reactions [16, 17]. Shape coexistence of exotic nuclei far from the stability line can result in several low-lying 0^+ states. Detection of electrons from the E0 transitions between the 0^+ states serves as a possible method to obtain more information about shape coexistence.

4.2 Types of Electron Spectrometers

Before the advent of the Si- and Ge-semiconductor detectors, the best energy resolution in nuclear spectroscopy was obtained by employing magnetic spectrometers in conversion-electron spectroscopy [18]. With these devices

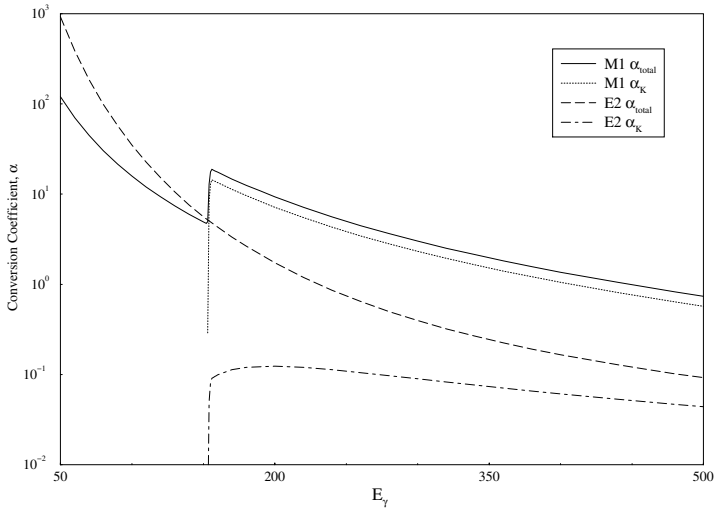

Fig. 7. Conversion coefficients for M1 and E2 transitions in Z = 103 nuclei. The electron conversion dominates for the M1 transitions with the transition energy below 400 keV and for the E2 transitions below 230 keV. It should be noted that for the M1 transitions the K conversion dominates as soon as the transition energy is above the K-binding energy while for the E2 transitions the L conversion dominates over the whole region

having a narrow momentum window only a small part of the energy spectrum at a time can be recorded. Most efficient of these spectrometers is the orange spectrometer, which has also been used in in-beam studies of heavy nuclei [19].

The range of 1 MeV electrons in silicon is about 2 mm and good energy resolution (below 2 keV) is obtained with a Si detector cooled to −20 °C. Therefore, the Si detectors are today the most commonly used in conversion-electron spectroscopy. However, due to other disturbing radiation, only in favourable cases, a bare Si-detector can be used to detect electrons directly from the source or target without combining it with an ancillary device.

The ancillary device normally used is a magnetic transporter to transport electrons to a Si detector situated in a less hostile environment further from a source or target. High transmission of electrons can be obtained by using a magnetic lens. The lens has a limited momentum window, but the current of the magnet coils can be swept to scan over the energy region of interest. In the lens spectrometer anti-positron baffles can be used to prevent positrons to hit the Si detector. Lens spectrometers have successfully been used also in in-beam studies of nuclei, which can be produced via a dominant reaction channel with relatively light projectiles [20].

Permanent magnets can be used to construct compact electron transporters. A mini-orange spectrometer consisting of several sheets of perma-

nent magnets was introduced by Van Klinken et al. [21]. The ICEMOS array of several mini-orange spectrometers was constructed by the Bonn–Saclay group [22]. It can be combined with various ancillary devices, like Ge-detector arrays, for in-beam measurements. The main problem with mini-orange spectrometers is the fixed momentum window and elimination of δ-electron background in in-beam measurements.

An electron spectrometer for collecting electron spectra of large energy range at a time (similar to the γ-ray measurements with Ge detectors) can be constructed if a strong solenoid magnet is used to guide electrons to a Si detector. The first solenoid spectrometer using normal magnetic coils was designed by Backe et al. [23]. Later the solenoid spectrometers typically used super-conducting magnets.

The main problem when using solenoid spectrometers in in-beam measurements is to prevent the vast amount of low energy atomic electrons (δ electrons) to hit the Si detector. They are induced by the projectiles hitting the target and their energy is increasing with increasing mass of the projectile ion. Therefore, the problem is severe especially when conversion electrons emitted from heavy-ion fusion reactions are detected. If the emission of the electrons of interest is delayed ($t > 100\,\mathrm{ps}$) a recoil-shadow method can be used: only the electrons emitted by the recoils flying out from a thin target are guided to the detector situated at ≈ 90 degree with respect to the beam direction while the prompt δ electrons hit a screen between the target and the detector.

4.3 SACRED – A Magnetic Solenoid Electron Spectrometer for In-Beam Measurements

A multipurpose broad-range electron spectrometer must be able to detect prompt conversion electrons within a wide energy range directly from the target. Such a solenoid-type of spectrometer equipped with a Si-PIN detector divided into 25 individual elements (SACRED), was designed and constructed by B. A. Butler et al. [24].

A section view of the latest version of the SACRED spectrometer used in a near-collinear geometry at the RITU recoil separator at JYFL is shown in Fig. 8 [25]. In this configuration the solenoid axis, tilted at an angle of 2.5 degrees with respect to the beam axis, crosses the beam axis at the target placed in a strong magnetic field. The beam passes a Si detector placed upstream of the target. Electrons emitted from the target into backward angles are guided by the solenoid field into the Si detector located in a region of weak magnetic field. In such away, electrons are distributed over the Si detector ($\oslash = 2\,cm$) which is divided into 25 independent pixels. Each of the pixels is equipped with individual amplifier and timing channels enabling to detect $e^- - e^-$ coincidences from a cascade of converted transitions. An important component of the spectrometer is the electrostatic HV barrier, which is designed to suppress the high flux of prompt low-energy δ electrons.

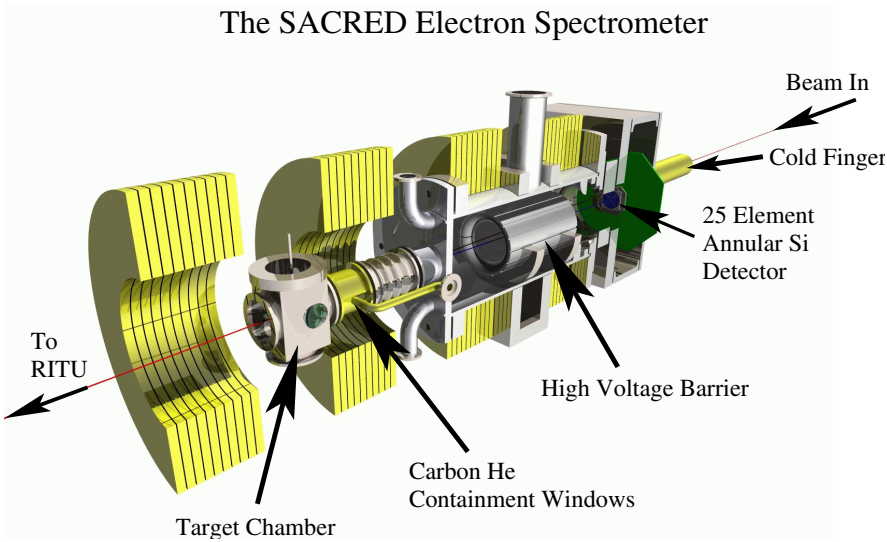

Fig. 8. A section view of the SACRED electron spectrometer designed for the use in conjunction with the RITU gas-filled recoil separator

5 Combined Systems

Powerful systems for nuclear spectroscopic studies of exotic phenomena and exotic nuclei have been constructed by combining high-resolution Ge detector systems with other selective devices.

5.1 Decay Spectroscopy

When the excited states of interest are populated in radioactive decay, decaying long-living nuclei can be transported further away from the hostile area of the production target by using ion guides and isotope separators or recoil separators. In case of β^- decay of neutron-rich nuclei, clean γ-ray spectra can be obtained by measuring γ rays in coincidence with β^- particles [26]. Similar measurements following β^+ decay of proton-rich nuclei are more difficult due to the 511 keV γ rays from annihilation.

Hindrance factors in the α decay give important information about nuclear structure. Especially in the region of very neutron deficient nuclei near the $Z = 82$ shell closure, fine structures of the α decay have been used to identify low-lying shape coexisting states [27]. Figure 9 demonstrates how γ rays measured in coincidence with α particles at the focal plane of the Recoil Ion Transport Unit (RITU) can be used to improve the energy resolution of 30 keV of α particles down to 2 keV of γ rays and to gain more information about the states fed in the α decay [28].

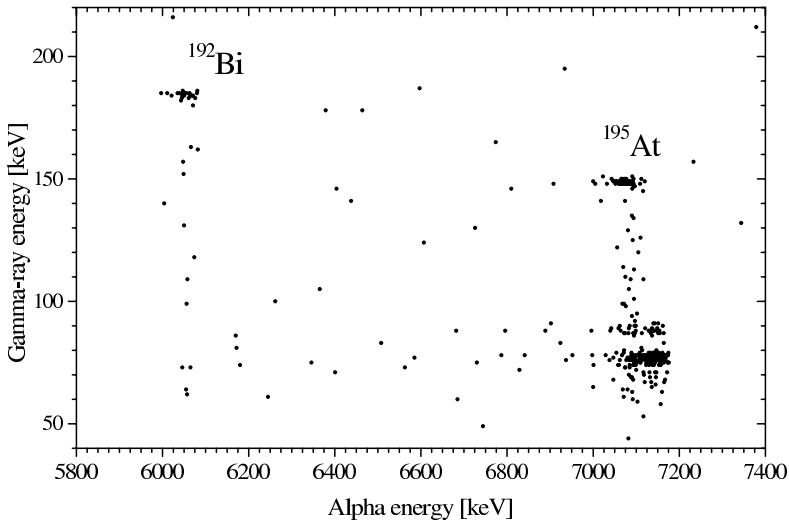

Fig. 9. An energy-energy matrix for γ-ray and α-particle concidences measured at the focal plane of the RITU recoil separator from residues of the ^{56}Fe + ^{142}Nd reactions. The strong X-ray peaks reveal the strong internal conversion of the 148 keV transition

5.2 In-Beam Spectroscopy with Ancillary Detectors

The first Ge-detector arrays were equipped with inner sum-energy or multiplicity-filter scintillation detector systems to enhance detection of high-multiplicity events from de-excitation of states at high spin [4]. In this way long cascades of γ rays from exotic rotational bands representing a yield of as low as 10^{-3} of the total fusion cross-section were observed. By detecting high-fold γ-ray coincidences with big arrays like EUROBALL or GAMMASPHERE, it has also been possible to resolve collective bands excited via very weak channels in transfer reactions in thick-target experiments [29]. If a thin target is used, the Doppler correction for γ rays emitted from heavy-ion induced transfer reactions or Coulomb excitation cannot be done without detection of the reaction products with a position-sensitive detector. Efficient Ge-detector systems combined with efficient position-sensitive gas counters for a detection of scattered ions have enabled comprehensive Coulomb-excitation studies of collective states of stable nuclei [30].

First steps towards in-beam studies of exotic neutron-deficient nuclei were taken when Ge-detector arrays were equipped with particle detectors for a detection of charged particles or/and neutrons evaporated in fusion reactions in coincidence with γ rays. The number of charged-particle evaporation channels increases with decreasing Z of the compound nucleus. Therefore, high-efficiency and high-granularity charged-particle detector arrays are today still the most powerful systems in channel selection when γ rays from neutron-deficient nuclei with $Z < 50$ are detected. The neutron detectors

(neutron wall) typically occupy the forward angles of the array [31], while for charged particles various types of inner detector balls surrounding the target are used [32]. Microball, an inner ball consisting of CsI scintillation detectors and combined with the GAMMASPHERE array, has been very powerful in γ-ray studies of light nuclei [33].

5.3 Recoil-Gating and Recoil-Decay-Tagging Methods

Disturbing background radiation, typically due to fission and Coulomb excitation, in in-beam spectroscopic studies of neutron deficient and heavy nuclei produced via fusion evaporation reactions, can be reduced if γ rays or electrons are detected in coincidence with evaporation residues. For such measurements a recoil separator is needed. Recoil separators are typically using magnets and electric fields but also systems like the Recoil Filter Detector designed by Heese et al. [34], which is based on the use of time-of-flight information, can be used.

Recoil separators. Reaction products from fusion-evaporation reactions are strongly focused along the beam axis. Therefore electromagnetic recoil separators with an acceptance covering a relatively small solid angle around the direction of the primary beam can be used for in-flight separation of evaporation residues from other types of reaction products as well as from the beam. The conventional recoil separators combine bending dipole and focusing quadrupole magnets and strong electric fields enabling mass/charge (m/q) selection of evaporation residues.

Conventional recoil separators suffer from different charge states of evaporation residues as in practice typically only two charge states can be collected by the focal plane detector (Fig. 10). The problem can be overcome by filling the active volume of the separator with dilute helium gas (or hydrogen), typically of 1 mbar in pressure. In the gas the recoiling reaction residues quickly (within few cm) reach an equilibrium charge state in such away that the separator actually is velocity and charge focusing. As a result, all the fusion evaporation residues entering the separator are focused on a spot at the focal plane which now can be covered by a single detector (Fig. 10). This results in high efficiency (high transmission, up to 50 %) of the separator but is done at the expense of mass resolution, which is basically lost.

Recoil gating. Mass information is especially needed in studies of medium-heavy and light nuclei when the fusion cross-section is distributed over several evaporation channels. For heavy nuclei the mass separation becomes more difficult, but on the other hand, due to the higher Coulomb barrier, the number of charged-particle evaporation channels in fusion reactions rapidly decreases with increasing Z.

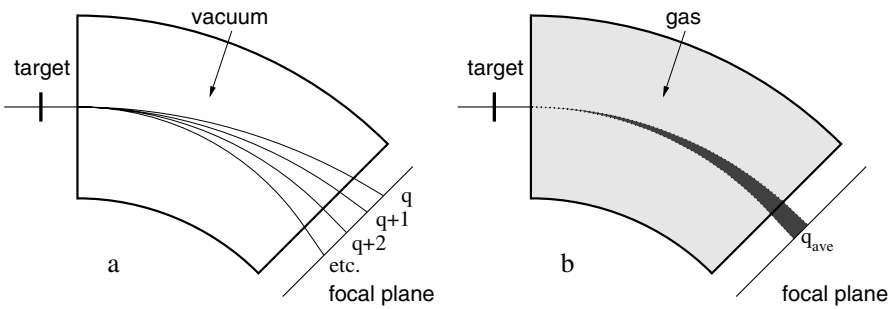

Fig. 10. Atomic charge-exchange collisions of recoiling ions in gas result in an average charge state of the ions and thus in a compressed distribution at the focal plane of the separator

The recoil separators were originally designed for focal-plane decay measurements of short living activities. These measurements are still playing an important role in studies of exotic nuclei and are often combined with in-beam γ-ray or conversion-electron measurements. For such studies the target area of the recoil separator is equipped with a γ-ray or conversion-electron spectrometer, respectively. The first in-beam measurements by using recoil gating of γ rays were carried out at the Daresbury Laboratory in the UK, where the RMS (Recoil Mass Separator) [35] separator was combined with TESSA type of Compton-suppressed Ge detectors. Detection of γ rays from an exotic N = Z nucleus ^{80}Zr showed that production limit of 10 μb can be reached in in-beam studies of such relatively light nuclei [36]. Similar measurements utilising m/q separation have been carried out at the Camel separator at the Legnaro Laboratory in Italy, where the GASP array was used for γ-ray detection [37]. The most productive in such studies has been the combination of the FMA (Fragment Mass Analyzer) separator and the GAMMASPHERE array at the Argonne National Laboratory (ANL) in the USA, where exotic light and heavy nuclei have been studied [38].

Recoil gating without m/q information is used in in-beam spectroscopic studies of heavy nuclei to resolve γ rays emitted by fusion-evaporation products from γ rays emitted in fission and Coulomb excitation of the target. Fission contribution quickly increases with increasing Z of the compound nucleus. For example, in an in-beam study of the neutron-deficient nucleus ^{171}Ir the maximum cross-section of 10 mb for the ^{144}Sm(^{36}Ar, p2n)^{171}Ir reaction was obtained with a beam energy of 267 MeV [39]. Fission of the compound nucleus ^{174}Pt at this energy represents a contribution of the order of 85 %. Gamma-gamma coincidence events gated with fusion evaporation residues were finally used to construct the level scheme of ^{171}Ir. Trans-fermium nuclei with Z close to 102, can be produced with cross-sections of 100–1000 nb in cold fusion reactions involving evaporation of one or two neutrons. In such cases, basically only one fusion reaction channel is open and therefore clean

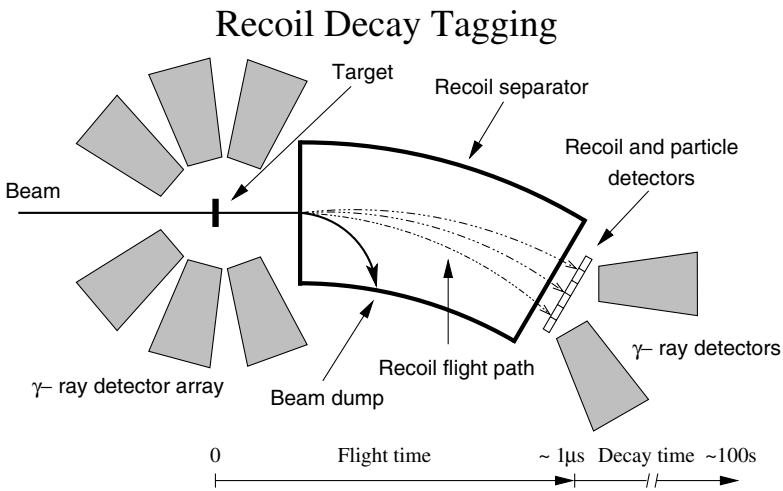

Fig. 11. In the Recoil-Decay-Tagging (RDT) method decay products of the reaction residue are measured at the focal plane of a recoil separator and used to identify prompt γ rays the residue has emitted at the target area

spectra of γ rays of interest can be obtained just by recoil gating (Sect. 7). The fission contribution in the decay of such a heavy compound nucleus is as high as 99.998 % ! The gas-filled separator like RITU at JYFL provides high transmission and is therefore well suited for recoil gating when m/q information is not needed [40].

Recoil-Decay-Tagging. Resolving power in in-beam spectroscopy experiments at recoil separators can further be improved if characteristic decay properties of reaction products detected at the focal plane of a separator can be used to identify nuclei of interest. For the first time, such a measurement was carried out at GSI in Germany by Simon et al. by using a set up of NaI(Tl) scintillation detectors at the target area of the SHIP recoil separator [41]. The name "Recoil-Decay-Tagging" (RDT) for this method was given by E. Paul et al., who carried out the first RDT feasibility measurement using the EUROGAM array at the RMS separator of the Daresbury Laboratory in the UK [42]. Later, successful RDT experiments have been carried out at ANL in Argonne with GAMMASPHERE at FMA and at JYFL in Jyväskylä with the JUROSPHERE array at the RITU separator (Chap. 6). So far, α and proton decays as well as γ rays emitted in de-excitation of isomeric states have been utilised in the RDT measurements.

A scheme illustrating the idea of the RDT method is shown in Fig. 11. Nuclei produced in the target de-excite mostly to the ground state by emitting γ rays (or conversion electrons). These prompt γ rays are detected by the detector array at the target area. The forward peaking reaction products from

fusion evaporation reactions flying out from the thin ($0.5\,\mathrm{mg/cm^2}$) target are separated from the beam and are focused on a recoil detector at the focal plane. For fusion evaporation reactions the velocity distribution of the recoiling product nuclei is narrow, resulting in a narrow time-of-flight distribution through the separator. Therefore, in spite of the recoil flight time through the separator, typically of the order of $1\,\mu\mathrm{s}$, a narrow coincidence window of typically 100 ns in the time distribution between the prompt γ rays and the detected fusion evaporation residues can be used. Angular distribution of fission fragments and other reaction products is more isotropic. Therefore, due to the small angular acceptance of the separator (typically of the order of 10 msr) only a small contribution of these products are detected at the focal plane.

At the focal plane, the recoils are distributed over the recoil detector which is a position sensitive Si detector or a Si detector segmented into small pixels. The recoil nucleus detected in a pixel is identified by observing its characteristic decay products (α particles or protons) in the same pixel. Detection of another recoil in the same pixel within the time interval between the detection of the recoil and its decay product results in a false event. Therefore, limits for the application of the RDT method are set by the lifetime of the nucleus of interest and the effective granularity (position resolution or number of the pixels) of the recoil detector. They set the limit for the allowable maximum recoil rate without any significant contribution of false random events. The effective granularity also takes into account the shape of the recoil distribution over the recoil detector.

Lifetimes of nuclei shorten when going further from the line of stability. Consequently, the RDT method is well suited for identifying γ rays from excited states of exotic short living nuclei. It is mostly used for probing structures of α decaying neutron deficient heavy and very heavy nuclei produced in fusion-evaporation reactions. In these cases the discrete α-particle peaks serve as an ideal tool to identify the recoil. Furthermore, for heavy nuclei the recoil rate at the focal plain is suppressed by the dominant fission contribution. As a consequence, no m/q information is needed in the identification, which enables to employ the high-transmission gas-filled recoil separator in such RDT measurements.

Gamma rays following de-excitation of an isomeric state and detected at the focal plane of a recoil separator can also be used to identify prompt γ-ray transitions feeding the isomeric state. So far it has not been demonstrated that β decay could be used to tag prompt γ rays, obviously due to the continuous character of the β spectrum and the lack of short living β-decaying nuclei.

6 In-Beam Spectroscopic Studies of Very Neutron Deficient Z ≈ 82 Nuclei at JYFL

The gas-filled recoil separator RITU was designed at JYFL originally for decay studies of heavy elements [40]. In RITU the recoiling fusion evaporation residues are implanted into a 80 mm × 35 mm Si strip detector covering about 70 % of the recoil distribution at the focal plane. The Si detector is devided into 5 mm wide vertical strips each having position resolution in vertical direction of about 0.4 mm. This position sensitivity enables the recoils to be correlated with their subsequent particle decay (α decay in the following examples), detected in the same pixel. High transmission of RITU makes it very suitable for γ-ray measurements in recoil-gating or RDT experiments. In most of the in-beam γ-ray experiments at RITU the JUROSPHERE array was used to detect prompt γ-rays at the target area. This array consisted of 25 Compton-suppressed Ge-detectors (15 EUROGAM Phase 1, 10 NORDBALL and TESSA detectors) and had a photo-peak efficiency of 1.7 % for 1.3 MeV γ rays. In addition, in most of the measurements 1–5 Ge detectors were used at the focal plane for detecting γ rays from transitions following isomeric or α decays. A picture of the spectrometer system is shown in Fig. 12.

6.1 Coexistence in Even-A Pb Nuclei Beyond the N = 104 Neutron Mid-Shell

Low-lying excited 0^+ states associated with deformed oblate proton 2p–2h and prolate proton 4p–4h intruder structures have been observed in Pb isotopes with N ≥ 102 [43–47,22,27]. In ^{186}Pb, the prolate and the oblate 0^+ states are the lowest excited states above the spherical ground state.

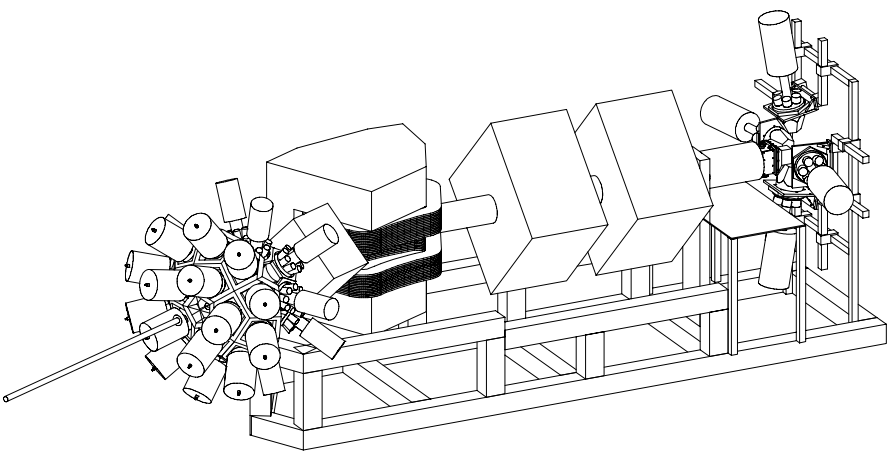

Fig. 12. The RITU separator combined with the JUROSPHERE array around the target

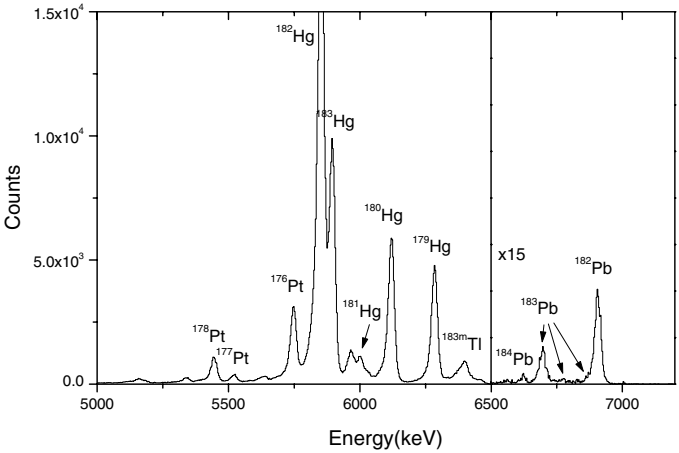

Fig. 13. Energy spectrum of α particles from ^{42}Ca + ^{144}Sm reactions observed within a 170 ms time interval after the detection of a recoil at the same position in the Si strip detector. The beam energy of 209 MeV was chosen to maximise the production of ^{182}Pb via the 4n channel. The spectrum demonstrates how the charged-particle evaporation channels are still the dominant ones

In in-beam experiments, low-lying deformed rotational structures have been observed at I $> 2\,\hbar$ in ^{186,188}Pb by Heese et al. [34], Baxter et al. [48] and Dracoulis et al. [49]. The RDT method was employed at JYFL to identify similar low-lying intruder bands associated with the prolate shape in ^{184}Pb [50] and in ^{182}Pb [51].

The ^{144}Sm(^{42}Ca, 4n) fusion evaporation channel was used to populate excited states of $^{182}_{82}$Pb$_{100}$. An α-particle energy spectrum observed at the RITU focal plane is shown in Fig. 13. From the recorded 3500 ^{182}Pb α-decays the extracted cross-section was only about 300 nb and the ^{182}Pb half-life $t_{1/2} = 64(7)$ ms in accordance with the earlier value of 55 ms [52]. Thanks to the short lifetime and low recoil rate of few tens per second, the RDT analysis resulted in a very clean energy spectrum of prompt γ rays shown in Fig. 14. The six lines marked in the spectrum are firmly assigned to originate from ^{182}Pb. The most intense 888 keV line obviously represents the $2^+ \rightarrow 0^+$ transition. The other five transitions clearly form a rotational cascade similar to those from the prolate bands built on the 2^+ states in ^{184,186,188}Pb and therefore, they are tentatively assigned as E2 transitions.

The number of neutrons in the nucleus ^{182}Pb is 26 less than in the double magic ^{208}Pb and it lies beyond the $82 < N < 126$ mid-shell close to the proton drip line. The observed members of the band have higher energies than those of the similar bands in ^{184}Pb and ^{186}Pb revealing that the prolate minimum lies lowest at N = 103.

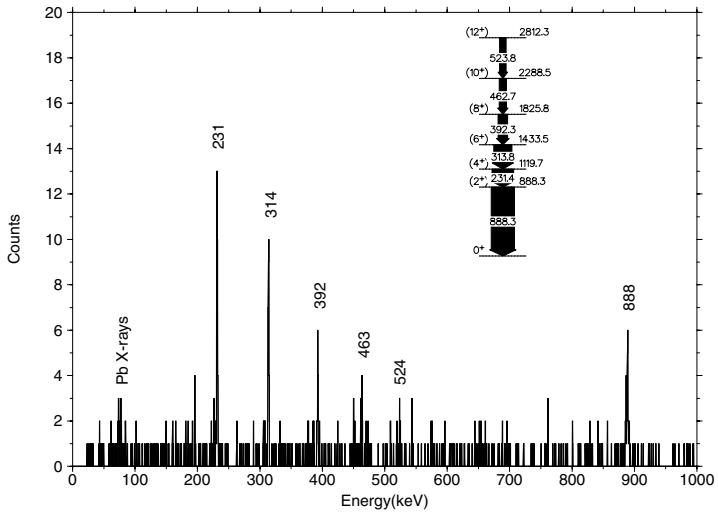

Fig. 14. A prompt γ-ray energy spectrum generated by gating with fusion evaporation residues from the ^{42}Ca + ^{144}Sm reaction and tagging with ^{182}Pb α decays. The level scheme of ^{182}Pb deduced from the present data is shown as an inset

6.2 Towards Prolate Po Isotopes

The first highlight in the series of successful RDT measurements at JYFL was the first observation of yrast transitions in ^{192}Po [53]. The spectra shown in Fig. 15 demonstrate the power of the RDT method. The regular pattern of peaks of Fig. 15c reveals that the deformed intruder structures, associated with oblate deformation, have become yrast and dominate in the ground-state configuration of ^{192}Po.

A more difficult RDT experiment was carried out at JYFL to observe yrast transitions in ^{190}Po [54]. A ^{142}Nd target was bombarded with a ^{52}Cr beam and excited states in ^{190}Po were produced via the 4n–fusion-evaporation channel with a cross-section of only about 200 nb. The ^{190}Po α decays were used to tag prompt γ rays resulting in a spectrum shown in Fig. 16. There are not many events in the spectrum but thanks to the very low background clear peaks are observed at 233, 299, 370, and 437 keV and possibly also at 485 keV. Based on the intensity behaviour and regularity of the γ-ray lines this pattern is associated with an yrast E2 cascade in ^{190}Po.

By combining this information with available data for heavier even-A Po isotopes, an energy-level systematics of the even-A Po nuclei shown in Fig. 17 is obtained. A sudden drop of the observed level energies is due to an oblate 4p–2h intruder band becoming yrast in ^{196}Po and reaching the ground state in ^{192}Po. However, the expected levelling off of the level energies when moving to ^{190}Po is observed only for the 2^+ states. For other higher-spin yrast levels another sudden drop of energies is seen, revealing another change in the structure of the yrast states in the even-A Po nuclei.

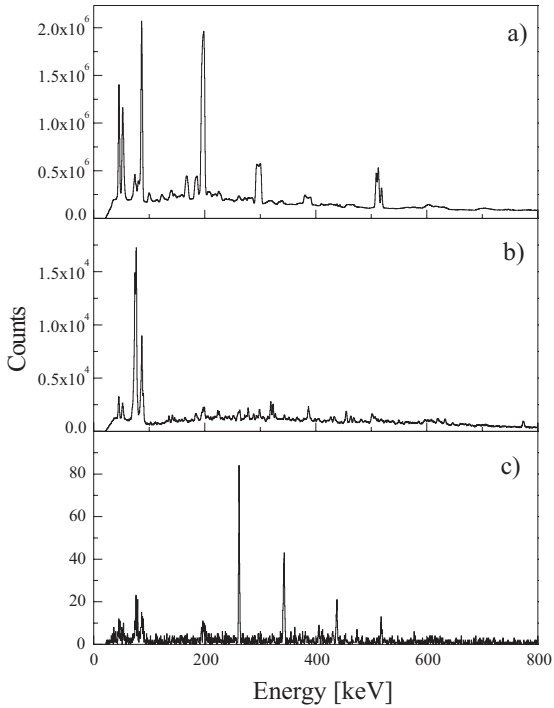

Fig. 15. Gamma-ray spectra from the ^{36}Ar (178 MeV) + ^{160}Dy reactions. (**a**) The singles spectrum is dominated by γ rays from fission and Coulomb excitation of the target. (**b**)The spectrum gated by separated recoils still do not show any peaks from ^{192}Po . (**c**) The γ-ray spectrum extracted by tagging with the α decay of ^{192}Po reveals the lines from the yrast transitions in ^{192}Po

In Fig. 18, values of the kinematic moment of inertia $J^{(1)} = \hbar^2(2\mathrm{I}-1)/E_\gamma$ as a function of γ-ray transition energy derived from the yrast level energies of the even-A $^{190-194}$Po nuclei are plotted with those for ^{186}Hg [57], ^{188}Pb [34] and ^{198}Rn [58]. The prolate bands in the mid-shell Hg and Pb nuclei are very similar. The $J^{(1)}$ values for ^{190}Po are very close to the values for isotones ^{186}Hg and ^{188}Pb showing that indeed, the yrast line of ^{190}Po represents a prolate structure very similar to the ones seen in Hg and Pb nuclei. The $J^{(1)}$ values for the oblate intruder yrast band of ^{192}Po and ^{194}Po are smaller and similar to the yrast band in ^{198}Rn indicating that similar oblate deformation as in Po nuclei sets in in light even-A Rn isotopes [59].

On the basis of the Po level systematics and mixing calculations [60] a 0_2^+ state should be the first excited state in ^{194}Po. This state could be missed in the γ-ray experiments. Therefore, an experiment was carried out at JYFL by employing the collinear SACRED magnetic solenoid spectrometer combined with RITU (Fig. 8 [25]) to detect prompt conversion electrons from the possible E0($0_2^+ \rightarrow 0_1^+$) transition. In the recoil-gated and α- tagged

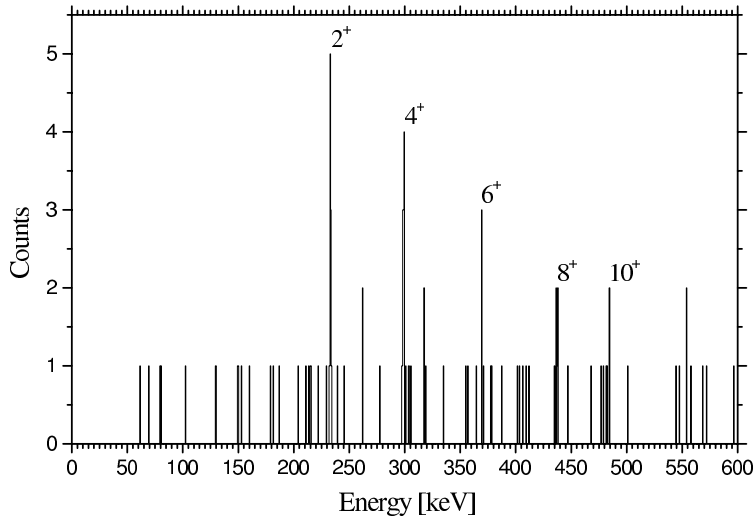

Fig. 16. An energy spectrum of prompt γ rays obtained by gating with fusion evaporation residues from the ^{52}Cr + ^{142}Nd reaction and by tagging with ^{190}Po α decays

electron spectrum from the ^{171}Yb(^{28}Si, 5n)^{194}Po reaction shown in Fig. 19, a candidate electron line is seen which could represent such an E0 transition from a 0_2^+ at about 220 keV in ^{194}Po [61]. More experiments are needed to confirm this result.

7 In-Beam Spectroscopic Studies of Transfermium Nuclei at JYFL

The Coulomb energy of the heavy nuclei with Z > 100 is so large that in the liquid drop picture these nuclei should be unstable against spontaneous fission. However, the nuclear shell-correction energy is large enough for creating an expected island of spherical super-heavy elements around Z = 114, N = 184. Moreover, the discoveries of α decaying new elements up to Z = 112 reveal that this island is not separated from the continent of known nuclei by the sea of fission as originally expected. The stability of these nuclei with Z > 100 is supposed to originate from the shell effects in a deformed nucleus. It is important to verify the predicted deformations experimentally. Current theoretical models give different predictions of the proton and neutron magic numbers beyond Z = 82 and N = 126. Detailed spectroscopic studies of the heaviest even- and odd-mass nuclei are therefore of importance in testing these models.

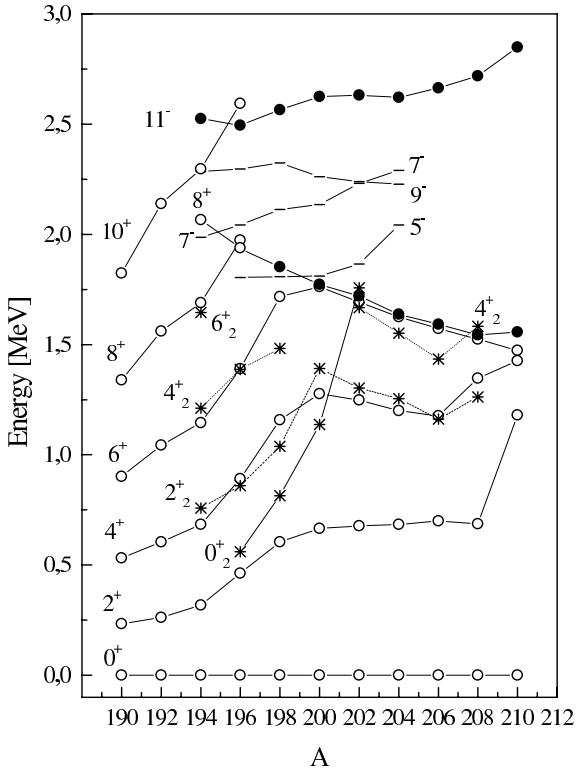

Fig. 17. Energy-level systematics for even-mass Po isotopes. The data for ^{190}Po, ^{192}Po and partially ^{194}Po are from the RITU+JUROSPHERE experiments. The other data have been taken from [55], and [56] and references therein. The open circles denote the positive parity yrast levels, the asterisks the non-yrast ones and the bars the negative parity levels. The isomeric states are denoted by the filled circles

7.1 Production Cross-Sections

The small production cross-sections make any kind of detailed spectroscopic studies of heavy elements extremely difficult. They are produced with available stable-isotope beams and targets in heavy-ion induced fusion-evaporation reactions. Due to fission, the production rates decrease rapidly with the proton number of the compound system, being down to 10 nb for example for the ^{40}Ar + ^{208}Pb reactions.

However, by using the doubly-magic projectile ^{48}Ca and Pb or Hg targets, exceptionally high cross-sections of cold fusion evaporation reactions are obtained. In particular, the fusion of two doubly magic nuclei in the ^{208}Pb(^{48}Ca, 2n) ^{254}No reaction leads to an anomalously high cross-section of about 2 μb providing a unique opportunity for an in-beam experiment on ^{254}No. In similar ^{48}Ca induced reactions on the ^{204}Hg and ^{206}Pb targets,

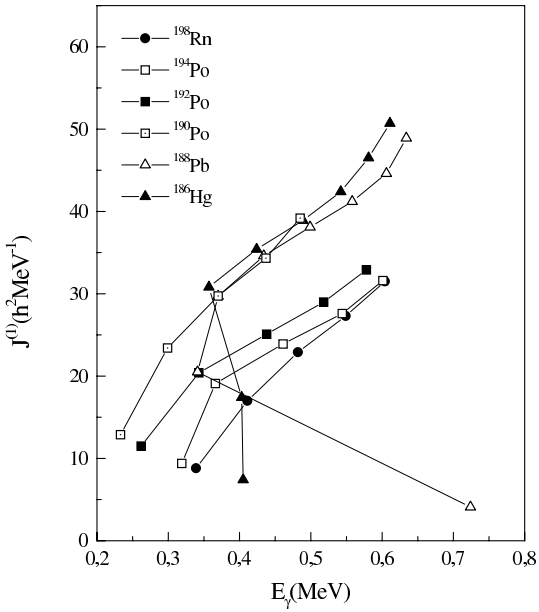

Fig. 18. Kinematic moments of inertia for the yrast line of the even-A $^{190-194}$Po nuclei compared to the ones for ^{186}Hg, ^{188}Pb and ^{198}Rn

^{250}Fm and ^{252}No are produced with cross-sections of 1000 nb and 300 nb respectively. Moreover, a unique feature of the cold fusion-evaporation reactions leading to this heavy mass region is that basically only one reaction channel, in this case the 2n channel is open, which makes the channel selection easy compared to that in lighter nuclei.

7.2 Prompt Gamma Rays from ^{254}No,^{252} No and ^{250}Fm

The first RDT measurement for ^{254}No at RITU was carried out by using the ^{208}Pb(^{48}Ca, 2n)^{254}No reaction and an array of 4 Clover detectors (SARI array) at the target area [62]. A resulting γ-ray spectrum gated with fusion products detected at the RITU focal plane is shown in the upper panel of Fig. 20. The lower panel shows a γ-ray spectrum in coincidence with fusion products identified as ^{254}No nuclei on the basis of recoil-α correlations. The half-life of ^{254}No is 55 s and therefore a maximum search time as long as 200 s was used. Such a long time interval between the detection of a recoil and its subsequent decay without any other recoil hitting the same detector pixel, is possible as the total recoil rate of the Si strip detector was about two per minute and the effective granularity of the detector is 200.

The two γ-ray spectra of Fig. 20 are very similar revealing the fact that the 2n channel is basically the only open channel. The photo-peak efficiency of the SARI array was 1.7 % when operated in add-back mode. The clover detectors

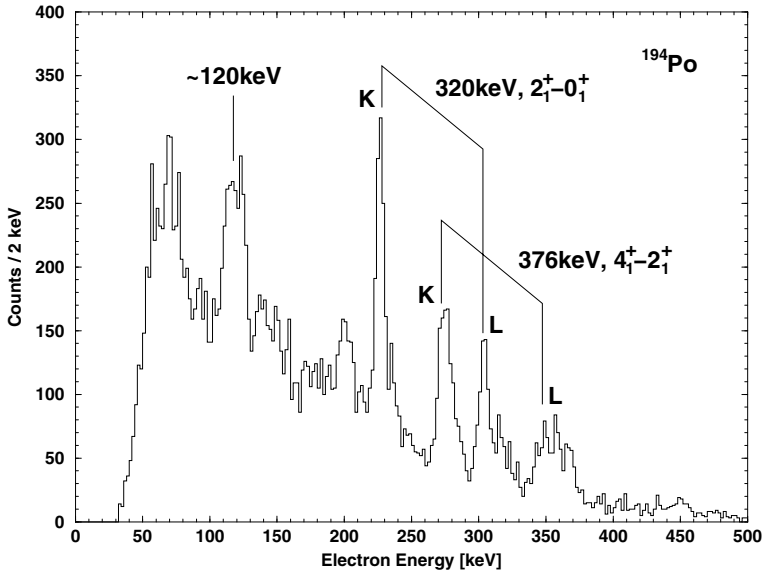

Fig. 19. Prompt conversion electrons from the ^{171}Yb(^{28}Si, 5n)^{194}Po reactions tagged with ^{194}Po α decays

didn't have any Compton-suppression shields and therefore the background in the spectra of Fig. 20 is significant compared to those obtained with the JUROSPHERE array.

In addition to the No X-rays, transitions having energies of 159, 214, 267, 318, 267 and 414 keV were observed and assigned to originate from ^{254}No. The first five of these transitions were observed, for the first time, in a similar tagging experiment at ANL [63]. The pattern of the γ-ray peaks in the spectra reveals that the corresponding transitions form a cascade, obviously of E2 transitions in ^{254}No. The spin assignments are based on a fit of the kinematic moment of inertia. Obviously, the γ-ray transitions from the states with $I < 6$ are not seen due to their internal conversion.

An experiment similar to that for ^{254}No was carried out for ^{252}No by using the ^{206}Pb(^{48}Ca, 2n)^{252}No reaction [64]. The recoil gated and RDT γ-ray spectra are shown in Fig. 21. The quality of these spectra is much higher than of those for ^{254}No in Fig. 20, albeit the reaction cross-section is only 300 nb. This is because the JUROSPHERE array with 25 Compton-suppressed Ge detectors was used.

The JUROSPHERE array was further employed in an RDT experiment to collect γ-rays from the ^{204}Hg(^{48}Ca, 2n)^{250}Fm reaction. Spectra similar to those for ^{252}No were obtained for ^{250}Fm. The observation of discrete γ-ray lines of a rotational cascade of transitions up to $I = 20$ in ^{254}No, ^{252}No and ^{250}Fm reveals that these trans-fermium nuclei are deformed and can compete against fission in rotation up to at least that spin. The kinematic

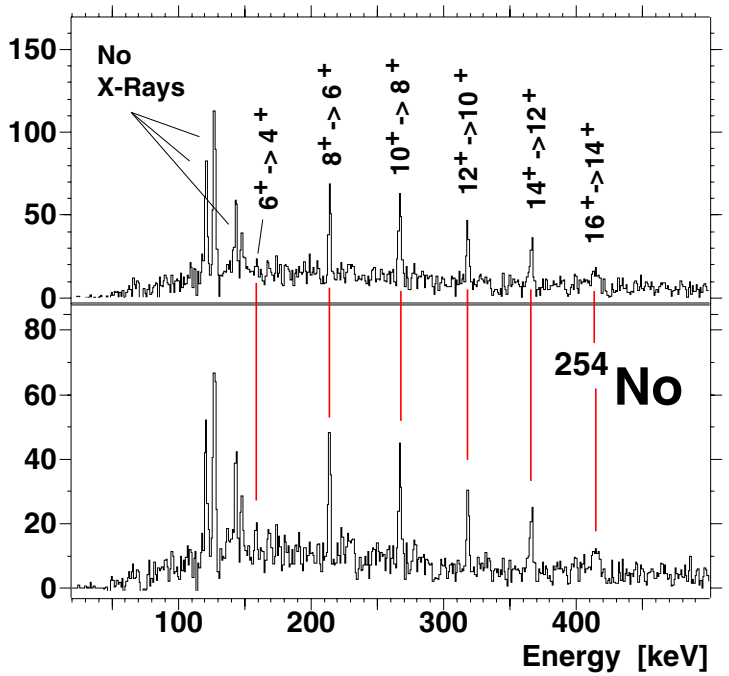

Fig. 20. A singles γ-ray spectrum (upper) from the ^{48}Ca + ^{208}Pb reactions gated with fusion-evaporation residues. The same γ-ray spectrum but in addition, tagged with the ^{254}No α decays (lower)

moment of inertia values for these nuclei derived from the observed transition energies are about half of the rigid rotor value and are slightly increasing with spin (Fig. 22), obviously due to gradual alignment of quasi-particles. For ^{252}No the extracted values increase more rapidly at high spin indicating a more dramatic alignment of quasi-particles. The kinematic moment of inertia values for ^{250}Fm are almost identical to the ^{254}No ones at low spin but then follow the alignment pattern of ^{252}No at higher spin. It is possible to extract the ground state deformation parameter β_2 from the extrapolated energy of the 2_1^+ state using global systematics [65,66]. The values derived for ^{254}No and ^{254}Fm are $\beta_2 = 0.27$, while ^{252}No is a bit less deformed with $\beta_2 = 0.26$.

7.3 Conversion Electrons from ^{254}No

The SACRED conversion-electron spectrometer in near collinear geometry described in Sect. 4.3. was used to measure prompt conversion electrons from the ^{208}Pb(^{48}Ca, 2n)^{254}No reactions [25]. In a resulting recoil gated spectrum shown in Fig. 23, electron peaks originating from transitions between the low-spin yrast states in ^{254}No are seen. In a careful analysis of the prompt recoil-gated electron-electron coincidence spectra it was found out that the

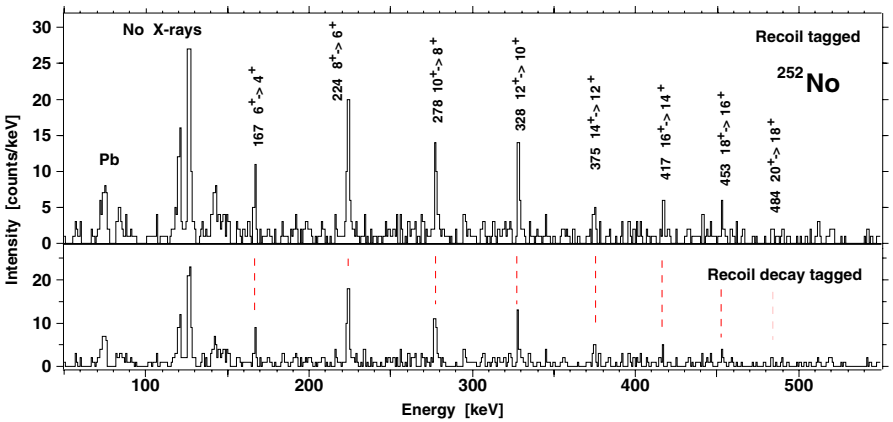

Fig. 21. A recoil gated singles γ-ray spectrum (upper) from the ^{48}Ca + ^{206}Pb reactions. The same spectrum but, in addition, tagged with the ^{252}No α decays (lower)

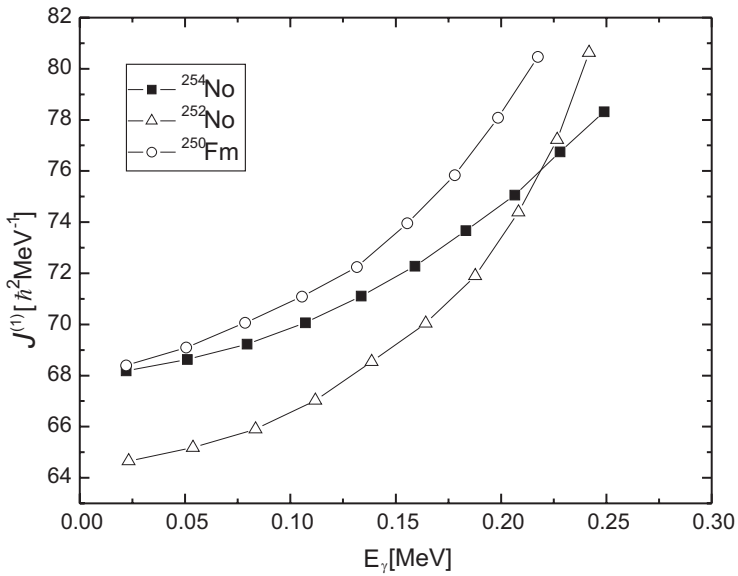

Fig. 22. Kinematic moments of inertia for ^{250}Fm, ^{252}No and ^{254}No extracted from the measured γ-ray energies

broad distribution under these electron peaks is not due to random events but consists of high-multiplicity events, obviously originating from cascades of highly converted M1 transitions within rotational bands built on high-K states in ^{254}No [67].

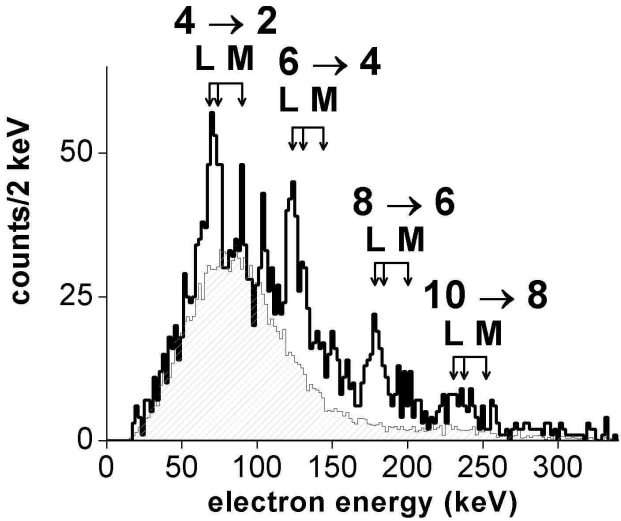

Fig. 23. A conversion-electron spectrum tagged by ^{254}No recoils. The hashed area shows a simulated spectrum of electrons from M1 transitions of high K bands in ^{254}No [67]

8 Summary and Outlook

Best energy resolution in probing structures of exotic nuclei is obtained by detecting γ rays with Ge detectors. Much effort has recently been focused on increasing detection efficiency of Ge-detector arrays by simultaneously maintaining good spectral properties. The new designs are based on the use of composite detectors with segmented Ge crystals. Such a state-of-the-art spectrometer is the EXOGAM array at GANIL consisting of 16 Clover detectors of segmented Ge crystals[10].

Pulse-shape analysis of the segment signals using digital electronics is the basis for a new concept, γ-ray tracking. The goal is to cover most of the 4π solid angle with Ge material and select full-absorption events by reconstructing tracks of individual γ rays. In addition, digital signal processing should enable an increase of the maximum tolerable counting rate of a Ge detector by a factor of ten, which so far is one of the most severe limitations in in-beam measurements. The ongoing projects for γ-ray tracking arrays and associated electronics are the joint-European AGATA project[14] and the GRETA project in the USA[12].

Existing conventional Compton suppressed Ge detectors have successfully been employed in studies of exotic nuclei when they are combined with recoil separators and other ancillary detectors. In the previous chapters it was shown how a relatively modest Ge-detector array JUROSPHERE was combined with the RITU gas-filled separator at JYFL to detect γ rays from nuclei produced with cross-sections as low as 200 nb in RDT measurements. Very

recently the JUROSPHERE array was replaced by a 4 % array, JUROGAM, consisting of 43 EUROGAM Phase 1 detectors and enabling to collect $\gamma\gamma$ coincidences in RDT studies of weakly populated nuclei. Moreover, a new sophisticated focal plane spectrometer GREAT comprising position sensitive recoil-, α-, electron- and γ-ray detectors was commissioned. Furthermore, a new type of Total Data Read out (TDR) data collection system, based on 10 ns stamping of signals of individual channels, was commissioned enabling efficient correlation of prompt and delayed signals from various types of detectors at the target and the focal plane.

Recent experiments employing the SACRED magnetic solenoid spectrometer at RITU show that in-beam detection of conversion-electrons from exotic nuclei produced at a level of 1 μb is also possible. One of the future goals is to combine a modular Ge-detector array and an electron spectrometer for simultaneous in-beam detection of γ rays and electrons from exotic heavy nuclei.

References

1. J. Blachot: Nuclear Data Sheets **92**, 455 (2001)
2. M. Jääskeläinen *et al.*: Nucl. Instr. Meth. **204**, 385 (1983)
3. V. Metag *et al.* In: *Detectors in Heavy-Ion reactions*, ed. by W. von Oertzen, Lecture Notes in Physics Vol. 178 (Springer-Verlag, Berlin, 1983) p. 163
4. P.J. Nolan, D.W. Gifford and P.J. Twin: Nucl. Instr. Meth. **A236**, 95 (1985)
5. P.J. Twin*et al.*: Phys. Rev. Lett. **57**, 811 (1986)
6. P.J. Nolan: Nucl. Phys. **A520**, 657c (1990)
7. D. Bazzacco In: *Proceedings of Workshop on Large gamma-ray Detector Arrays*, Chalk River, Canada, (1992), AECL-10613, p. 376
8. I.Y. Lee: Nucl. Phys. **A520**, 641c (1990)
9. J. Simpson: Z. Phys. **A358**, 139 (1997)
10. J. Simpson: APH N.S. Heavy Ion Physics **11**, 159 (2000)
11. J. Eberth *et al.*: Prog. Part. Nucl. Phys. **38**, 29 (1997)
12. K. Vetter *et al.*: Nucl. Instr. Meth. **A452**, 223 (2000)
13. Th. Kröll and D. Bazzacco: Nucl. Instr. Meth. **A463**, 227 (2001)
14. AGATA Proposal, ed. by J. Gerl and W. Korten (2001)
15. R. D. Page *et al.*: Nucl. Instr. Meth. **B204**, 634 (2003)
16. J. Kantele: 'What can we learn from E0 transitions and how ?' In: *Heavy Ions and Nuclear Structure*. ed. by B. Sikora and Z. Wilhelmi (Harwood Academic, London, 1984)
17. R. Julin: Physica Scripta **T56**, 151 (1995)
18. G.T. Ewan, R.L. Graham In: *Alpha- and Beta-and Gamma-Ray Spectroscopy*, ed. by K. Siegbahn (North-Holland Publ. Co., Amsterdam 1965) p. 951
19. T. Wendel *et al.*: Phys. Rev. **C65**, 014309 (2002)
20. J. Kantele: *Handbook of Nuclear Spectroscopy* (Academic Press, London 1995) p. 213
21. J. Van Klinken *et al.*: Nucl. Instr. Meth. **130**, 427 (1975)
22. Y. Le Coz *et al.*: Eur. Phys. J. (Direct) **A3**, 1 (1999)
23. H. Backe *et al.*: Z. Phys. **A285**, 159 (1978)

24. P.A. Butler *et al.*: Nucl. Instr. Meth. **A381**, 433 (1996)
25. H. Kankaanpää: In-Beam Spectroscopy of Very Heavy Elements. PhD Thesis, University of Jyväskylä, Research Report No. 8 (2001)
26. J. Äystö *et al.*: Nucl. Phys. **A525**, 365 (1990)
27. A.N. Andreyev *et al.*: Nature **405**, 430 (2000)
28. H. Kettunen *et al.*: Eur. Phys. J. **A16**, 457 (2003)
29. J. Cocks *et al.*: Phys. Rev. Lett. **78**, 2920 (1997)
30. C. Fahlander *et al.*: Nucl. Phys. **A485**, 327 (1988)
31. S.E. Arnell *et al.*: Nucl. Instr. Meth. **A300**, 303 (1991)
32. E. Farnea *et al.*: Nucl. Instr. Meth. **A400**, 87 (1997)
33. D.G. Sarantites *et al.*: Nucl. Instr. Meth. **A381**, 418 (1996)
34. J. Heese *et al.*: Phys. Lett. **B302**, 390 (1993)
35. A.N. James *et al.*: Nucl. Instr. Meth. **A267**, 144 (1988)
36. C. J. Lister *et al.*: Phys. Rev. **C42**, R1191 (1990)
37. P. Spolaore *et al.*: Nucl. Instr. Meth. **A359**, 500 (1995)
38. C.N. Davids *et al.*: Nucl. Instr. Meth. **B70**, 358 (1992)
39. R.A. Bark *et al.*: Nucl. Phys. **A657**, 113 (1999)
40. M. Leino *et al.*: Nucl. Instr. Meth. **B99**, 653 (1995)
41. R.S. Simon *et al.*: Z. Phys. **A325**, 197 (1986)
42. E.S. Paul *et al.*: Phys. Rev. **C51**, 78 (1995)
43. P. Van Duppen *et al.*: Phys. Rev. Lett. **52**, 1974 (1984)
44. P. Van Duppen *et al.*: Phys. Rev. **C35**, 1861 (1987)
45. J.L. Wood *et al.*: Phys. Rep. **215**, 101 (1992)
46. N. Bijnens *et al.*: Z. Phys. **A356**, 3 (1996)
47. R. Allatt *et al.*: Phys. Lett. **B437**, 29 (1998)
48. A.M. Baxter *et al.*: Phys. Rev. **C48**, 2140 (1993)
49. G.D. Dracoulis *et al.*: Phys. Rev. **C67**, 051301 (2003)
50. J.F.C. Cocks *et al.*: Eur. Phys. J **A3**, 29 (1998)
51. D.G. Jenkins *et al.*: Phys. Rev. **C62**, 021302(R) (2000)
52. K.S. Toth *et al.*: Phys. Rev. **C60**, 011302(R) (1999)
53. K. Helariutta *et al.*: Phys. Rev. **C54**, R2799 (1996)
54. K. Van de Vel *et al.*: Eur. Phys. J. **A17**, 2 (2003)
55. L.A. Bernstein *et al.*: Phys. Rev. **C52**, 621 (1995)
56. R.B. Firestone *et al.*: *Table of Isotopes*, 8th edn. Vol. II (John Wiley & sons inc., New York 1996)
57. W.C. Ma *et al.*: Phys. Rev. **C47**, R5 (1993)
58. R. Taylor *et al.*: Phys. Rev. **C59**, 673 (1999)
59. R. Julin, K. Helariutta and M. Muikku: J. Phys. G: Nucl. Part. Phys. **27**, R109 (2001)
60. K. Helariutta *et al.*: Eur. Phys. J. **A6**, 289 (1999)
61. P. Rahkila: JYFL Annual Report 2001, p.14
62. M. Leino *et al.*: Eur. Phys. J. **C6**, 63 (1999)
63. P. Reiter *et al.*: Phys. Rev. Lett. **82**, 509 (1999)
64. R.-D. Herzberg *et al.*: Phys. Rev. **C65**, 014303 (2001)
65. L. Grozins: Phys. Lett. **2**, 88 (1962)
66. S. Raman *et al.*: At. Data Nucl. Data Tables **42**, 1 (1989)
67. P.A. Butler *et al.*: Phys. Rev. Lett. **89**, 202501 (2002)